Polymer 56 (2015) 20–28

Contents lists available at ScienceDirect

Polymer

journal homepage: www.elsevier.com/locate/polymer

Polyurethane-silica hybrid foam by sol–gel approach: Chemical and functional properties

Letizia Verdolotti [a], Marino Lavorgna [a, *], Raffaele Lamanna [b], Ernesto Di Maio [c], Salvatore Iannace [a]

[a] Institute of Polymers, Composites and Biomaterials, National Research Council (IPCB-CNR), P.le E. Fermi 1, 80055 Portici, Na, Italy
[b] Biotec-Agro CR ENEA Trisaia, SS 106 Jonica Km 419.5, 75026 Rotondella, Mt, Italy
[c] Dipartimento di Ingegneria Chimica, dei Materiali e della Produzione Industriale, University of Naples Federico II, P.le Tecchio 80, Italy

ARTICLE INFO

Article history:
Received 29 July 2014
Accepted 5 October 2014
Available online 24 October 2014

Keywords:
Hybrid polyurethane foams
Polysiloxane domains
Thermal conductivity

ABSTRACT

Hybrid foams based on polyurethane and polysiloxane-domains were designed in terms of chemical structure and hierarchical morphology to improve the thermal insulation capability of conventional polyurethane foams. Polysiloxane-domains by sol–gel approach reacted with polyols to produce a polysiloxane-reactive-adduct, which completed its formation into polysiloxane aerogel-like structure during the polyurethane foaming process. Hybrids with 5wt% of the polysiloxane-domains exhibited a 22% reduction in thermal conductivity in comparison with pristine PUR. The chemical structure and the hierarchical morphology were studied by means of SAXS/WAXS and ^{29}Si and ^{13}C NMR. In particular the hybrid structure consisted of coarse polysiloxane-fractal-aggregates composed of silica nanoparticles embedded in the polyurethane matrix. Morphological analysis revealed a decrease of the cell size with the increase of the siloxane content ascribed to the nucleation effect of polysiloxane-domains during the foaming. The cell size reduction and the formation of hybrid-aerogel-like structures within the cell-walls are considered the key factors to reduce the thermal conductivity of hybrid foams.

1. Introduction

Organic–Inorganic hybrid materials by sol–gel approach represent a growing and attractive area of nano-engineered materials because of their promise to provide specific peculiarity and multifunctional alternatives to conventional-filled plastics [1,2]. Hybrid materials includes a wide range of materials, rom single-phase polymer networks, where the hybrid composition refers to the presence of functional groups of different nature with respect to the main component [3], to self-assembling or host-guest superstructures, characterized by co-continuous organic and inorganic phases [4]. Several epoxy and polyimides hybrids materials have been produced by using different routes based on the sol–gel approach exhibiting improved hardness and solvent resistance, thermo-mechanical stability as well as mechanical properties [5,6]. In this context the preparation of polyurethane-silica hybrid foams represents a viable route to improve many properties of conventional polyurethane foams, particularly thermo-mechanical stability [7]. However, the key property of the polyurethane foams (PUR) is the thermal conductivity which needs to be significantly reduced in order to both expand and make sustainable the application fields of PUR foams. In particular, the improvement of insulation properties of PUR is mainly addressed to the necessity of a more effective insulation of buildings or devices like refrigerators to save energy and reduce CO_2 emissions. The thermal conductivity of polymeric foams is modeled as the sum of several contributions [8–10]: a) conduction through the solid phase; b) conduction through the gas-filled interior; c) convention within the cells; d) radiation through the cell walls. The conduction through the solid phase contribution to the overall thermal conductivity is generally in the range of 10% for PUR because of polymeric phase has intrinsically low thermal conductivity (i.e for the polyurethane it is approximately 0.25 W/(m·K)) [9–11], and it occupies only a small fraction of the total volume of the foam. The convection contribution is negligible for cell size smaller than 4 mm, as confirmed by the Skochdopole experiment [11–13]. The radiation contribution is a significant part of the thermal conductivity of the foam (i.e it accounts for approximately 30% of the measured effective conductivity at room temperature) as indicated by Hyliard et al. [14] and Glicksman et al. [15]. The main contribution to the overall

* Corresponding author. P.le E. Fermi 1, 80055 Portici, Na, Italy. Tel.: +39 0817758838.
E-mail address: mlavorgn@unina.it (M. Lavorgna).

http://dx.doi.org/10.1016/j.polymer.2014.10.017
0032-3861/

conductivity of the foam is actually the conduction in the cell by the gas mixture. Gases with low thermal conductivity such as chlorofluorocarbons (CFC), might reduce this contribution, but were banned for their environmental effects. Furthermore, concentration gradient driven flows tend to bring air in the cells, in the place of the blowing agent, thereby inducing a progressive increase of the conductivity during the operation life of the foamed products.

Silica aerogels are highly insulating materials alternative to polymeric foams. This is an ultra-lightweight, open-celled, mesoporous material consisting of cross-linked silica nanoparticles with a huge volume of pores [16]. Silica aerogels have an overall thermal conductivity of 0.017 W/(m K) at ambient pressure, which is significantly lower than the thermal conductivity of the best performing polyurethane foams (i.e. thermal conductivity approximately equal to 0.026 W/(m K)). The low thermal conductivity of aerogels results from the combination of low solid skeleton conductivity, low gaseous conductivity and low radiated infrared transmission contribution [17]. In particular, in the aerogel material, the gaseous phase, which consists of air and occupies up to 90% of the volume, is compartmentalized in domains having sizes smaller than the diffusion mean free path of air. This contributes to severely reducing the thermal conductivity [18].

However, the inherent fragility and the environmental sensitivity (e.g., hygroscopicity) of silica aerogels, have restricted their use to extreme applications such as space applications. In order to overcome these limitations and to promote the application of silica aerogel in the thermal insulating of buildings and refrigerators, several attempts have been made to produce aerogels crosslinked to the organic polymers (i.e. X-aerogels). In particular, the mesoporous inorganic structure is crosslinking through organic moieties which constitute the necks between silica particle able to absorb deformation energy [19,21]. Typically, the structure of X-aerogels is obtained from a sol–gel process by using several silanol source (TMOS, TEOS, GOTMS etc) and base catalysts, followed after gelling by supercritical fluid extraction (CO_2) for fast extraction of the solvent [20–22]. Solvent exchange, where the polymer cross-linked silica aerogel monoliths is dried under ambient pressure by using solvent such as acetone, THF, pentane, is an alternative to supercritical fluid extraction [23].

To enhance the thermal insulating capability of PUR, then, it is possible to form the highly insulating aerogel-like materials directly during the polyurethane foaming process. In fact, the formation of organic-inorganic hybrids in the cell wall and struts introduces a large fraction of empty volume, which contributes to lower the heat transfer within the cell wall with respect to the pure material. In addition, it interrupts solid conductivity through the cell walls [24]. Similar approach realized through the use of particulate silica, especially silica aerogel, formed before polyurethane foam expansion, was proposed in 1994 by BASF Corporation [25].

In this work, the polyurethane-silica aerogel-like foams is produced through a preliminary preparation of polysiloxane domains by sol–gel approach in the presence of conventional polyols and subsequently through the foaming process during the reaction of the polyisocyanate with the obtained adducts of polysiloxane domains-modified polyols. Foams were obtained by changing the polysiloxane content, reported in the formulations as SiO_2 amount, in the range from 1.5wt% to 7wt%. The hybrid foams were characterized in terms of both chemical interactions established between polysiloxane and PUR and morphology by NMR, SAXS and SEM analysis. The results confirm that the thermal conductivity of hybrid foams decreases with the increase of the polysiloxane content as a consequence of both the decrease of foam cell size and the formation of a highly insulating organic-inorganic polyurethane aerogel-like material.

2. Experimental

2.1. Materials

Polyether polyol, with catalysts and silicone surfactants, was kindly provided by Huntsman (Daltofoam© TA 34300, $\eta = 4590$ mPa*s @ 25 °C; $\rho = 1.093$ g/cm^3 @ 25 °C). Suprasec© 5025 isocyanate (MDI) was also kindly provided by Huntsman (Italy). For the preparation of the polysiloxane domains, TEOS (tetraethylorthosilicate), HCl (chloridric acid) and distilled water were used. *n*-pentane, supplied by Aldrich (Italy), was used as the physical blowing agent. Silicone surfactant (L-6164) as cells stabilizer, ammine 1,3,5-Tris[3-(dymethylamino)propyl]-s-hexahydrotriazine (C41) and CH_3COOK as catalysts of both blowing and polymerization reactions were kindly supplied by Momentive (Germany).

2.2. Methods

2.2.1. Hybrid foams preparation

The stages of the hybrid foams preparation are as follows (see Scheme 1 where a schematic representation of the several stages for the production of hybrid foams is reported). For the preparation of polysiloxane domains (A in Fig. 1) we followed the procedure proposed by K. Zou et al. [26]. A mixture of TEOS 48.6%, ethanol 43.0%, water 8.4% by weight and $9.73 \cdot 10^{-4}$ mL of HCl per solution gram were mechanically mixed at room temperature for 24 h. During this stage, the TEOS hydrolyzes in silanols, which condense to siloxane adducts according to the well-established reactions of hydrolysis and condensation [27]. Afterwards, the hydro-alcoholic solvents were partially removed, using a rotary evaporator, at 60 °C, under vacuum at 50 rpm. The obtained hydroalcoholic polysiloxane liquor, equals to approximately 1/7 by weight of the TEOS-ethanol-water mixture, is characterized by a hydroalcoholic content of less than 15% by weight. Addition of this liquor to the polyol (in the amount to obtain 1.5, 3, 5 and 7% of SiO_2 by weight of the whole polyurethane formulation) with some additives (i.e. CH_3COOK and L6164, each of them 1% by weight of the polyol) and *n*-pentane (13% by weight of the polyol) (B in Fig. 1). Addition of the C41 surfactant (i.e 2% by weight of the polyol) to the isocyanate precursor (C in Fig. 1). Finally, both the polyol modified with polysiloxane domains and the isocyanate precursor were mixed by hand and poured into the mold for foaming (D in Fig. 1). The expansion was conducted into a rectangular mold, 360 × 200 × 40 mm, which was closed right after the start of the expansion. It was found that the higher the reactive polysiloxane amount, the slower was the foaming of hybrid polyurethane. After polymerization and foaming, the panels were removed from the mold. A panel of pristine polyurethane foam was also produced for proper comparison.

In Table 1, the formulations of pristine PUR and hybrid foams were reported.

2.3. Characterization

2.3.1. Nuclear Magnetic Resonance spectroscopy (NMR)

To investigate the chemical interactions between the polysiloxane and the polyurethane matrix NMR characterization was performed. NMR spectra were collected by using a 600 Avance Bruker spectrometer under magic angle spinning (MAS) conditions. ^{29}Si spectra where acquired by a 45° excitation pulse, 3280 scans, a spinning rate of 6 KHz and a recycle time of 80 s. The top of sample rotor was filled with a small amount of 2,2-dimethyl-2-silapentane-5-sulfonic acid, DSS for frequency calibration. ^{13}C single pulse experiments where performed spinning the samples at 11 KHz, to reduce spinning sideband (SSB) superposition with

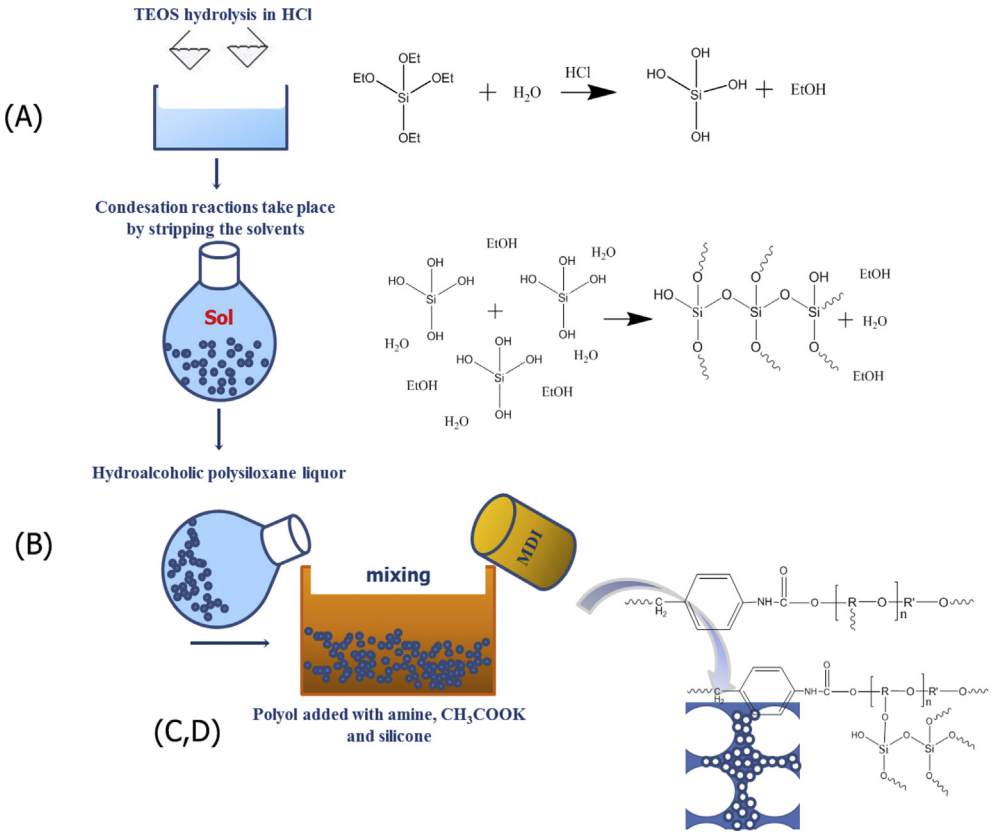

Scheme 1. Schematic representation of the several steps for the preparation of hybrid foams.

sample resonances, and under proton decoupling co-adding 12K spectra with a recycle time of 5 s. ^{13}C CPMAS spectra where acquired by using a ramp crosspolarization pulse with a contact time of 2 ms, 12 scans, a recycle time of 4 s, and a spinning rate of 6 KHz. All the spectra were acquired at the temperature of 25 °C.

2.3.2. Wide and Small Angle X-ray Scattering (WAXS/SAXS)

Structural characterization of PUR and hybrid materials was performed through simultaneous Wide (WAXS) and Small Angle X-ray Scattering SAXS analyses by using an Anton Paar SAXSess camera equipped with a 2D imaging plate detector. 1.5418 Å wavelengths CuKα X-Rays were generated by a Philips PW3830 sealed tube generator source (40 kV, 50 mA) and slit collimated. Spectra of pristine PUR and hybrid PUR (HPUR-1.5, HPUR-3, HPUR-5, HPUR-7) were collected for 10 min. All scattering data were dark current and background subtracted, and normalized for the primary beam intensity [26,28,29].

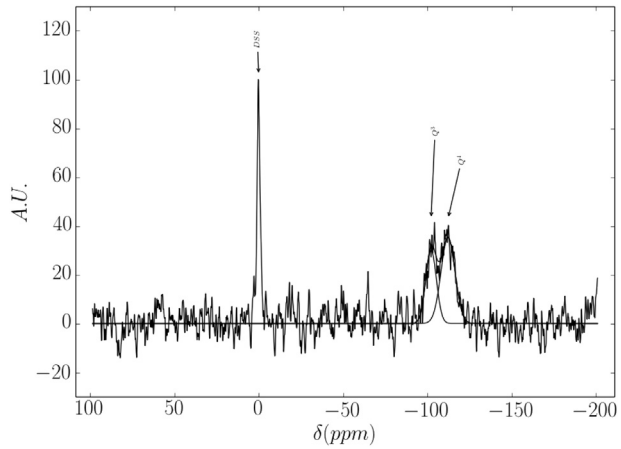

Fig. 1. ^{29}Si NMR spectrum of HPUR7 sample. Two Gaussian curves are also reported.

2.3.3. Morphological investigations

Scanning electron microscopy (SEM, type Leica S440) was used to observe the morphology of the hybrid foams. The sample to be investigated was cut with a sharp blade, to prevent cell walls twisting. A thin layer of gold was sputtered on the fracture surface of specimens, prior to SEM investigation. The average cell radius and the cell strut thickness were measured for each of the hybrid foams.

2.3.4. Thermal conductivity and content of closed cells

Thermal conductivity, λ was measured according to EN12667 (thermofluximeter method). The instrument was Lasercomp Fox 314. The ΔT between the two surfaces was 10 °C (in details, the upper surface was at 10.02 °C and the bottom surface was at 20.01 °C). The calibration material consisted of a glass fiber panel. The room temperature was 22 ± 3 °C and the relative humidity was 50 ± 10% HR. The content of closed cells was measured according to ASTM D2856.

2.3.5. Thermo-gravimetric analysis (TGA)

Thermo-gravimetric analysis (TGA) was carried out in nitrogen flow (flow rate = 40 ml/min) using a TGAQ500, TA Instruments at heating rate of 10 °C/min in the temperature range from 30 to 900 °C. Samples mass was approximately 10 mg.

Table 1
Pristine and hybrid polyurethane foams formulations.

Chemical	Samples				
	Pure-PUR [g]	HPUR-1.5 [g]	HPUR-3 [g]	HPUR-5 [g]	HPUR-7 [g]
Polyol	100	66.2	63.4	53	57
MDI	156	107.7	107.7	116.5	108.4
n-pentane	15	10.3	10.3	8.1	8.5
H_2O	1	Carried by the reactive silica source			
C41	–	1.32	1.27	1.05	1.14
L6164	–	0.66	0.63	0.53	0.57
CH_3COOK	–	0.66	0.63	0.53	0.57
Polysiloxane liquor[a]	–	6	12	20	28

[a] Liquor of polysiloxane precursors after solvent removal.

2.3.6. Mechanical properties, compression tests

The mechanical properties of the specimens were investigated by ASTM D1621 protocol [30]. The tests were carried out by using a, Shenzhen Sans (China), model CMT 4304, dynamometer equipped with a 1 kN load cell. Tests were performed at room temperature, by using specimens size 51 × 51 × 30 mm × mm × mm and at crosshead velocity equal to 3.61 mm/min.

Mechanical properties (elastic modulus, yield stress, yield strain, compressive strength, plateau stress, densification strain) were reported as average values of five tests for each material. Apparent densities were measured as the ratio between the foams weight (as measured with analytical balance) and the geometrical volume (as measured by a high-resolution caliper). Six specimens were tested for each composition.

3. Results and discussion

3.1. Chemical characterization: NMR analysis

The structure of polysiloxane domains into the hybrid PUR can be investigated by ^{29}Si MAS NMR. Despite the low sensitivity of ^{29}Si nuclei and the low percentage of polysiloxane in the hybrid samples, a quantitative spectrum can be obtained. The ^{29}Si single pulse spectrum of HPUR-7 sample is shown in Fig. 1 with the Gaussian deconvolution of the sample resonances. Only two signals are observed and attributed to Q^4 and Q^3 silicate structures [31,32]. The relative amount of the two silicate structures is estimated in 60% for Q^4 and 40% for Q^3.

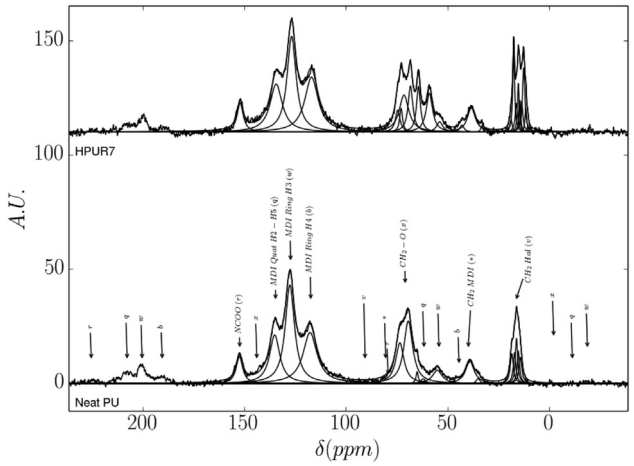

Fig. 2. ^{13}C single pulse proton decoupled spectra of neat PU and HPUR7 samples. The spectra are deconvoluted by Lorentzian curves. Line assignment is also reported with associated spinning sidebands.

Structures of the type $Si(O)_3R$, indicated as T [31], are not detected in the ^{29}Si spectrum. However, by fitting the largest noise peaks it is possible to estimate that the T structures are less than 5% of the total polysiloxane content.

The linkage between polysiloxane domains and polyurethane chains can be actually analyzed by ^{13}C NMR. In Fig. 2, the single pulse, proton decoupled ^{13}C MAS spectra of pristine PUR and HPUR-7 samples are reported, together with a deconvolution in Lorentzian components.

The MDI ring and urethane carbons are well identified in both samples between 100 and 150 ppm.

In the pristine polyurethane, the $-OCH_2-$ band presents three signals, while the aliphatic methylene band needs at least five Lorentzians to be correctly deconvoluted. This implies the presence of a quite complex CH_2 chemical environment. In the presence of polysiloxane, both $-OCH_2-$ and allylic $-CH_2-$ bands become more complex with an increased number of resonances. This could be due either to a shift of CH_2 resonances or to the addition of oligomers of polysiloxane to the –OH groups of polyols according to the following reaction scheme:

The integration of the resonance bands, by summing the areas of appropriate Lorentzian components, is reported in Table 2. The

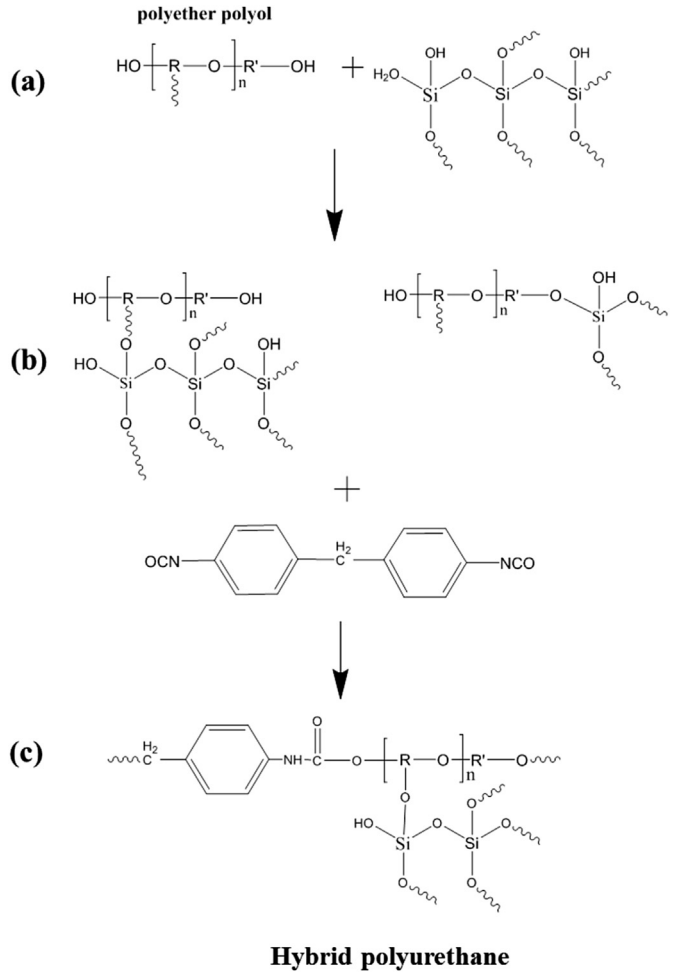

results confirm that the reaction between polyol and polysiloxane domains, which likely takes place before the addition of MDI, induces a change of the chemical environment of $-CH_2-$ groups with a significant modification of the resonances bands. The ^{13}C NMR

Table 2
Integral of polyurethane bands. The MDI-NCOO integral are arbitrarily posed to 14 which correspond to the number of carbons in these groups in each polyurethane monomer.

Samples	MDI + NCOO	OCH_2	CH_2-MDI	Hal-CH_2
Pristine PUR	14	2	1	1
HPUR7	14	3	1	2

results allow excluding the existence of any reactions between the isocynate groups and the silanols groups that are present on the surface polysiloxane domains.

The analysis of CPMAS spectra of all the hybrid foams, which are reported in Fig. 3, shows the separation of samples into two groups: samples having an amount of silicate between zero and 3% and samples with a higher amount. This evidence confirms the existence of an effect due to the amount of the polysiloxane domains on the hierarchical structuring of the inorganic phase as following proved by SAXS and SEM results (see following sections).

3.1.1. Morphological characterization: SAXS, WAXS and SEM analysis

WAXD spectra of pristine PUR and hybrid materials are shown in Fig. 4. It is noteworthy that: a) all of the systems are amorphous and b) the polysiloxane domains affect the shape of the polyurethane amorphous band with an increase of the scattering intensity at higher q values. Since the content of polysiloxane domains is low, i.e only a few units per cent by weight, this effect is ascribed to a modification of the local microstructure of the polyurethane network, which likely arises from the ability of polysiloxane domains to become involved in the building up of the organic network through condensation reactions between −SiOH groups and −OH groups of polyols, as confirmed by NMR analysis. Similar results were obtained for epoxy resins modified with silsesquioxane structure produced by sol–gel approach [33].

Additional information regarding the hierarchical structure and particle size and distribution of polysiloxane domains within the hybrids was obtained from SAXS measurements. The hierarchical structure of the polysiloxane domains can be deduced by adopting the Multiple Structural Level Model of Beaucage et al. [34] which assumes that experimental scattering profiles consist of multiple length scales (Guinier regimes) separated by power-law scaling regimes (Porod regimes). The Guinier regimes account for the

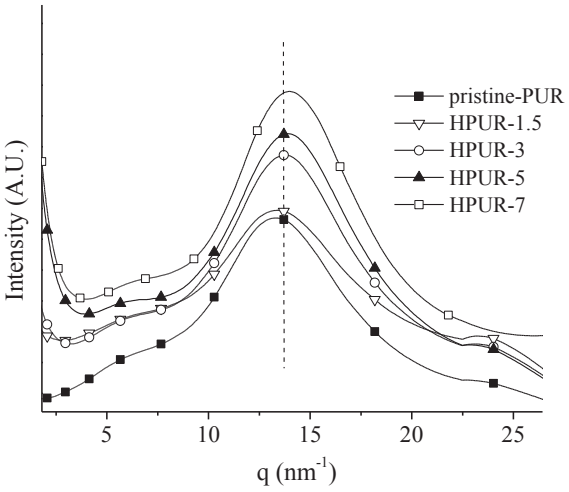

Fig. 4. WAXD spectra of pristine PUR and hybrid foams.

several length scales which constitute the hierarchical structure of the inorganic domain while the Porod regimes give information about the surface or mass of the fractal object. This approach has been widely applied to get insights into scattering data for organic-inorganic hybrids containing *in situ* generated siloxane domains by sol–gel approach [35]. From the log–log plot of SAXS spectra, it is possible to deduce important morphological parameters such the gyration radius, R_g which gives a measure of the mean square distance of the scattering centers from the centre of gravity and the fractal dimension, D_m as a measure of the compactness of the inorganic domains [33,36].

In Fig. 5, the SAXS spectra in the form of log–log plot for the inorganic component of hybrid samples are shown. In details, this diffraction contribution was isolated by SAXS spectrum of hybrid materials by subtracting the spectrum of pristine polyurethane after normalization for the sample thickness.

All of the spectra in Fig. 5 show the simultaneous presence of a knee diffraction feature coupled with a line diffraction region. This can be related to the presence of polysiloxane domains with a hierarchical structure. In particular, primary polysiloxane particles aggregate to form coarse fractal structures. The primary particle diameter, as evaluated according to Guinier's relation [26,28,29] from the gyration radius, R_g, is equal to 0.7–0.8 nm, slightly

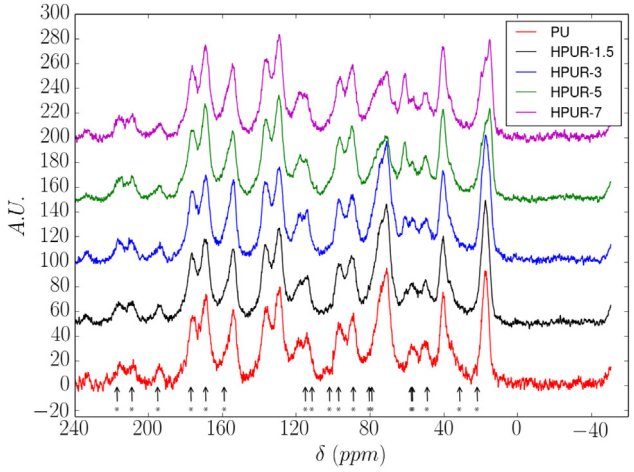

Fig. 3. ^{13}C CPMAS spectra of polyurethane and hybrid materials at different amounts of silicate. The position of spinning sidebands is indicated by arrows.

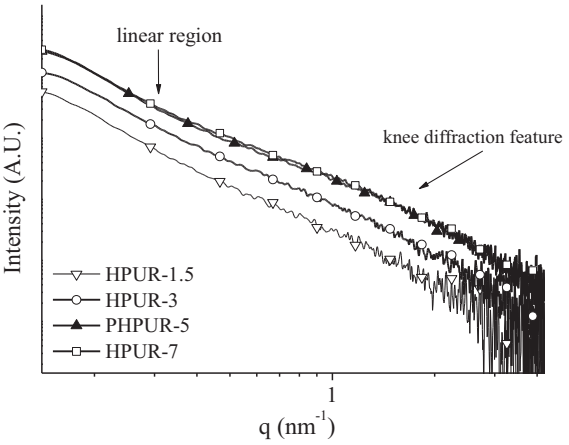

Fig. 5. SAXS spectra of polysiloxane aerogel-like structures present inside hybrid foams.

increasing with the polysiloxane content. The slope of the Porod region is in the range 2.8–3 for all the polysiloxane structures. This confirms that the primary polysiloxane particles aggregate to form spherical fractal aggregates.

From the spectra comparison, it can be deduced that the hierarchical polysiloxane structure does not change with the polysiloxane content in the hybrid foams. However, a slight difference is observed for the polysiloxane structure isolated from PUR hybrids with siloxane content lower than 3%wt. Indeed, with increasing silica content, a slight reduction of the q value at which the linear Porod region starts can be observed. This means that as the siloxane content increases as the primary polysiloxane domains become larger. This result is consistent with the results found in the literature, wherein it is reported that, in PUR materials doped with silica, the nanoparticles aggregation occurred at concentration higher than 3 wt% [25,37].

In conclusion, the process brings about the formation of polysiloxane nanoparticles that aggregate to form spherical, coarse polysiloxane domains. The size of the latter is larger than 50 nm (the maximum that could be detected with the SAXS alignment used), consisting of very dense fractal domains. This structure is compatible with the presence of voids entrapped in between the primary particles and the coarse fractal polysiloxane domains.

In Fig. 6, a schematic representation of the hierarchical polysiloxane morphology generated through the sol–gel approach carried out directly in the polyurethane matrix is reported. The hybrid foams have been observed by Scanning Electronic Microscopy in order to evaluated specific parameter such as average diameter of the cells as well as thickness of the walls between the cells. The results of the measurements are reported in Table 3. The normal distribution of the cell radius is shown in Fig. 7. The average cell radius decreases with increasing amount of the polysiloxane domains: in particular, the average cell radius of HPUR-5 is ca. 33% smaller than the average cell radius of pristine PUR. This confirms that the polysiloxane adducts act as a nucleating agent during the foaming process, promoting the formation of more numerous and smaller cells. Apparently, it also brings about a reduction of the cell strut thickness.

Selected SEM image of the cross-section and cells surface of pristine polyurethane and HPUR-5 foams are shown in Fig. 8. The presence of polysiloxane domains in the cross-section of cell struts modifies the rupture mechanism of the materials and the surface appears as constituted by coarse globular grains, well distributed throughout the wall thickness (see Fig. 8a and b). Indeed, the SEM images of the surfaces clearly show the presence of polysiloxane domains in the polyurethane matrix (see Fig. 8c and e). The red

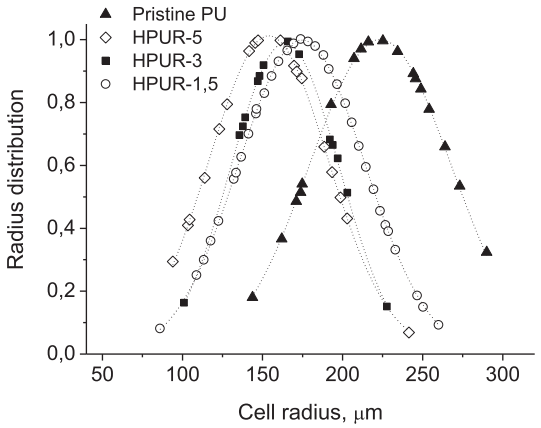

Fig. 7. Normal distributions of cell radius of the polyurethane foam and hybrid foams.

Table 3
Cell radius and cell strut thickness measured using SEM electronic microscopy, closed cell content.

Samples	Cell radius [μm]	Cell strut thickness [μm]	Closed cells average [%]	λ [mW/m K]
Pristine PUR	229 ± 10	47 ± 3	72.4	30.88
HPUR-1.5	172 ± 5	35 ± 5	74.7	29.10
HPUR-3	169 ± 8	30 ± 2	82.8	28.90
HPUR-5	152 ± 5	32 ± 2	70.0	24.19

*Sample HPUR-7 don't analyze because friable.

circles (in web version) evidence the polysiloxane domains homogeneously distributed in the polymer matrix, these appear as formed by smaller domains aggregated to form coarser domains. The SEM images confirm the existence of fractal domains embedded in the polyurethane matrix, as shown by SAXS analysis. Preliminary TEM observations have shown the existence of polysiloxane nanoparticles in the range of 1 nm sized (data not shown for brevity), which have been identified as the primary particles constituting the fractal aggregates.

3.1.2. Physical characterization: thermal conductivity and thermal-gravimetric analysis

The closed cell content and thermal conductivity, λ for pristine PUR and hybrid foams are reported in Table 3.

The results show that λ decreased by increasing polysiloxane content up to have a reduction of 22% for HPUR-5 with respect to

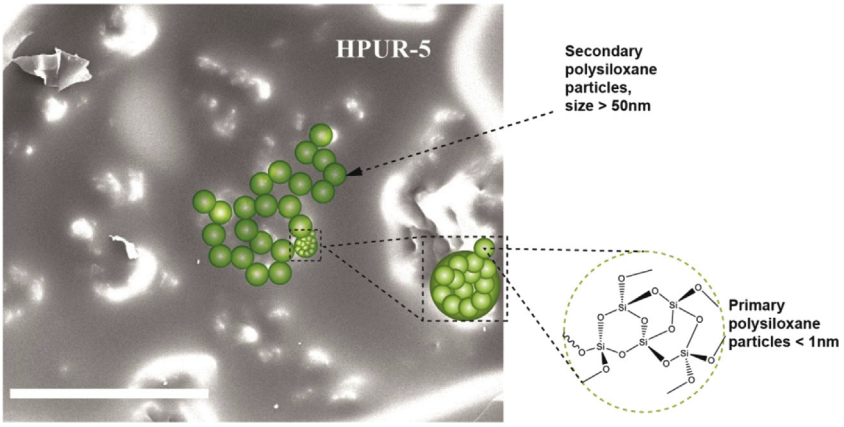

Fig. 6. Schematization of hybrid morphology with the aerogel-like structure.

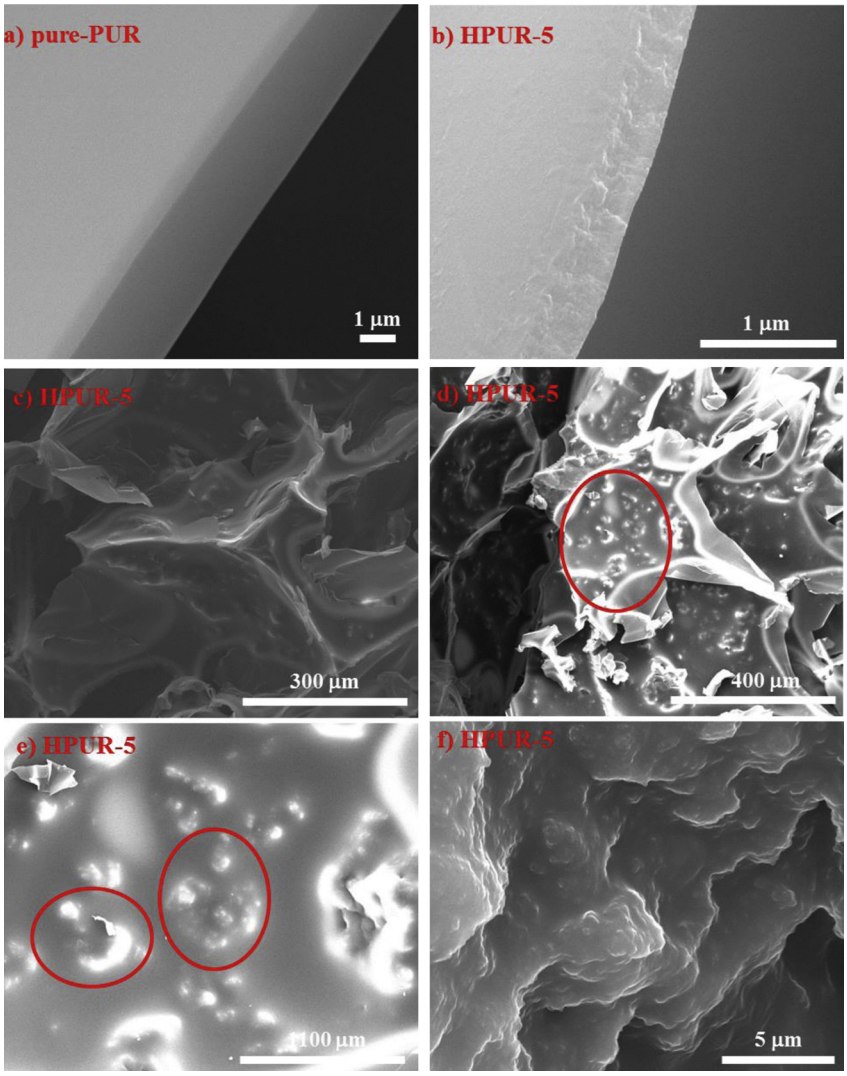

Fig. 8. SEM micrographs of pristine PUR and HPUR-5 at different magnifications.

the pristine PUR foams. This result is consistent with some those reported in the literature for foam composites filled with preformed aerogel particles. For instance, Okoroafor et al. and Biesmans et al. [25,38] found that the thermal conductivity of composite foams was at least 10% lower than that of unfilled polymer foam. Similar results have been recently obtained by Chang et al. [7], who investigated the effects of co-precursor method and the solvent exchange method for the preparation of silica aerogel. According to Okoroafor et al. [25], the addition of little amount (i.e. 0.1 wt%) of silica aerogel in presence of polysiloxane/polyoxyalkylene surfactants may significantly improve the insulating capability of polyurethane foams.

The decrease of the thermal conductivity with increasing polysiloxane is ascribed to both the reduction of the cell size due to nucleating effect of polysiloxane domains and the formation of the hybrid materials with fractal polysiloxane domains entrapping air. Thus, it may be assimilated to aerogel systems according to the chemical results described before.

The closed cell content reduced with the increase of polysiloxane content, apparently in contrast with the corresponding reduction of the thermal conductivity. In fact, open cells should contribute to the increases the thermal conductivity. However, Gibson and Ashby verified that closed cell content influences the thermal conductivity to a lesser extent than cell size [11]. In our case, the increment of open cells, detected according to the ASTM D2856 standard, is an evidence of the formation of the hybrid aerogel-like structure characterized by reduced thermal conductivity.

TGA thermograms for pristine PUR and hybrid PUR are shown in Fig. 9. In the thermogram of pristine PUR, two degradation steps can be observed. The first degradation step occurs in the range 200–425 °C (maximum of the derivative weight loss at 310 °C) with a weight loss equal to 67 wt% and, according to literature [37], can be ascribed to the breaking of urethane links leading to the production of CO_2, alcohols, amines, aldehydes, CO. The second degradation step occurs in the range 440–540 °C (maximum of the derivative weight loss at 475 °C) with a 15% weight loss, resulting from the chain scission of the polyol [37,39]. Hybrid foams, conversely, show three degradation steps. The first step weight loss (ranging 22–15wt%) occurs in the temperature range 200–290 °C and is attributed to elimination of water molecules due to the condensation reactions within the polysiloxane phase. The second step and the third step of mass loss (ranging 40–48 wt% and 15–8.7 wt% respectively) take place in the range 290–360 °C and 420–540 °C respectively and they are attributed to the polyurethane decompositions described before [39]. As summarized in

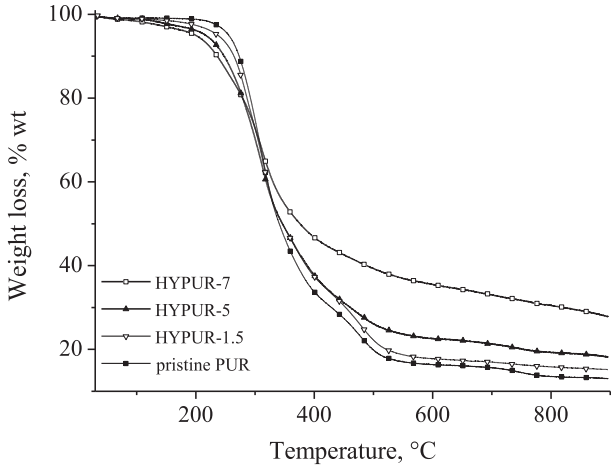

Fig. 9. Thermograms patterns for pristine PUR and hybrid foams.

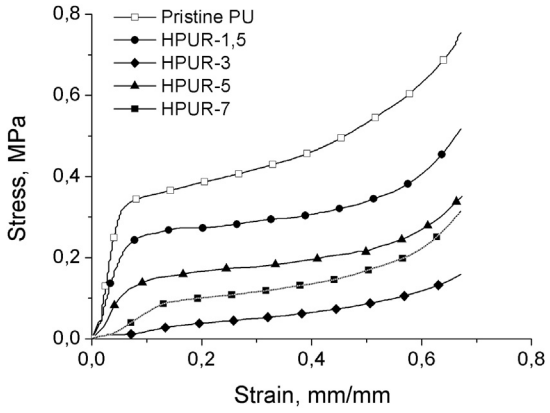

Fig. 10. Stress strain curves for pristine and hybrid foams.

Table 4, the maximum decomposition temperatures (T_2 and T_3) of the hybrid systems compared to the pristine PUR, increase with increasing polysiloxane content. At high polysiloxane contents (i.e. 5 and 7 wt%) the weight loss detected in the second degradation step is considerably reduced, confirming that a chemical modification of polyol structure has occurred due to interaction with polysiloxane domains. The enhancement of thermal stability can be ascribed to the presence of inorganic polysiloxane structure, which reduce the amount of more-combustible organic components and produce siliceous residues barrier layers that inhibit heat and mass transfer. Similar results were observed by Xia and Larock in waterbone castor oil-based polyurethane nanocomposites, where the presence of 0.5, 1 and 3% of silicon domains induced an increasing of onset decomposition temperatures of about 10 °C [37]. Finally, Nikje et al. [40] noted that in polyurethane foam materials doped by silica nanoparticles the temperature corresponding to 50% decomposition with increasing of nano silica shifted to higher temperatures.

3.1.3. Mechanical characterization

The stress-strain diagrams for pristine PUR and hybrid foams compression tests are shown in Fig. 10.

Typically, stress–strain curves of plastic foams in compression along the foam rise direction, show three characteristic phases: an initial linear elastic response, followed by a post-yield plateau and a final sharp rise. As a matter of fact we did not observe any horizontal plateau in the stress-strain curves, but the stress keeps increasing with the strain. Since the occurrence of the plateau is related to the cell walls/struts buckling, in our case the compressive behavior evidences an absence of morphological uniformity (uniform struts buckle at similar stresses). Furthermore, the densification does not bring about a sharp rise of the curve. Again, also in the final stage, since the morphology is not uniform, the densification occurs more gradually. The compressive tests results are summarized in Table 5. Because of the aforementioned difficulty in evidencing the plateau stress, the compressive yield point was obtained be means of the "tangent method": the tangent to the elastic part and to the post-yield part was drawn, and the abscissa of their intersection gave the compressive yield strain and the corresponding ordinate was the yield stress.

The elastic modulus, the compressive strength and the yield stress decrease with increasing the filler content (up to a 90% reduction for the HPUR-7 with respect to the pristine PUR). On the contrary, the yield strain increases with increasing the filler amount, up to more than 100% increment for HPUR-5. The reduction of the stiffness with the amount of filler can again be ascribed to the presence of hybrid structure in the strut of the cells: the fractal aggregates consisting of nanometric particles interrupt the polyurethane continuity and perturb the ordered sequence of the cell layers. In the literature, it was reported that the addition of preformed silica nanoparticles (up to 3% by weight) to polyurethane foam did not elicit such an abrupt decrease of the mechanical properties, but in some cases it even brought about an improvement of the stiffness [11,37,41]. In our case, we ascribe the observed reduction of the stiffness to the different way the polysiloxane domains have been obtained here, in-situ, and the corresponding observed extensive change in the chemical structure as proven by the chemical and morphological characterization. We can conclude that the reduction of the mechanical properties is due to both the presence of an aerogel structure within the cell wall and to the modification of the molecular architecture of the polyurethane, induced by the sol–gel approach employed to prepare the hybrid foams presented in this work.

4. Conclusions

This paper is focused on the preparation of hybrid PUR with polysiloxane domains obtained by sol–gel approach and on the enhanced thermal properties with respect to pristine PUR. The polysiloxane domains reacted with polyol precursor before the

Table 4
Decomposition temperature and mass loss of the hybrid foams.

Samples	T_1 [°C]	Weight loss wt%	T_2[°C]	Weight loss wt%	T_3[°C]	Mass loss wt%
Pristine PUR	–	–	309.5	67.4	480	15
HYPU-1.5	285	22	317	40	480	15.9
HYPU-3	281	22	321	42	480	14.2
HYPU-5	280	19.4	313	45.7	481	8.6
HYPU-7	245	15.5	311	48	479	8.7

Table 5
Young's modulus, compression strength, yield stress and yield strain of the hybrid.

Samples	Young's modulus [MPa]	Compression strength [MPa]	Yield stress [MPa]	Yield strain [MPa]	Density [kg/m^3]
Pristine PUR	8.2 ± 1.0	0.34 ± 0.02	0.32 ± 0.02	0.05 ± 0.01	62 ± 1
HPUR-1.5	6.1 ± 0.6	0.26 ± 0.01	0.25 ± 0.01	0.05 ± 0.01	62 ± 1
HPUR-3	2.8 ± 0.4	0.14 ± 0.01	0.13 ± 0.01	0.06 ± 0.01	56 ± 1
HPUR-5	0.9 ± 0.2	0.07 ± 0.01	0.07 ± 0.01	0.11 ± 0.03	63 ± 1
HPUR-7	0.3 ± 0.1	0.03 ± 0.01	0.02 ± 0.01	0.10 ± 0.02	73 ± 1

foaming reaction. Subsequently, during the addition of isocyanate precursor the temperature increment alongside with the presence of pentane allow stripping the mixture of hydro-alcoholic solvents produced by hydrolysis and condensation reactions of siloxane, leaving a fractal structure with voids. This structure can be assimilated to an aerogel crosslinked to the polyurethane matrix.

The hybrid foams exhibit a significant reduction of the thermal conductivity which reduces linearly with the increment of polysiloxane domains. In order to investigate the formation of the polyurethane hybrid structure, the hybrid foams were studied from the chemico-physical, mechanical and functional point of view. NMR investigations highlighted the presence of interactions between the polysiloxane domains and the polyol, precursor of polyurethane matrix. SEM electronic microscopy revealed a decrease of the cell size with increasing reactive filler amount: this effect contributed to enhance the insulation properties, probably together with effect related to the formation of fractal aggregates constituted by polysiloxane domains aggregated to form fractal structure. Their presence was observed by means of SAXS and WAXS scattering and was considered to be the key parameter for the reduction of thermal conductivity. Because of the increased crosslink density imparted by the formation of an inorganic nanostructure bonded with polyurethane phase, hybrid foams showed higher thermal stability than neat polyurethane as well as a significant decrement of mechanical properties. This work represents a first contribution in the field of polyurethane hybrid foams with the presence of polysiloxane assimilated aerogel produced in-situ by sol–gel approach. Further developments are in progress and mainly addressed to the obtainment of hybrid foams with enhanced thermal insulation properties alongside with satisfatying mechanical properties.

Acknowledgment

We are grateful to Enza Migliore for drawing support.

References

[1] Mascia L. In: Functional fillers for plastics. Weinheim: Wiley-VCH; 2010. p. 459–68.
[2] Mascia L, Lavorgna M. In: Wiley encyclopedia of composites. New York: VCH; 2012. p. 1922–41.
[3] Cardiano P, Sergi S, Lazzari M, Piraino P. Polymer 2002;43:6635.
[4] Russo L, Gabrielli L, Valliant EM, Nicotra F, Jimenez-Barbero J, Cipolla L, et al. Mater Chem Phys 2013;140:168–75.
[5] Abbate M, Musto P, Ragosta G, Scarinzi G, Mascia L. Macromol Symp 2004;218:211–20.
[6] Mascia L, Prezzi L, Lavorgna M. Poly Eng Sci 2005;45:1039–48.
[7] Chang K-J, Wang Y-Z, Peng K-C, Tsai H-S, Chen J-R, Huang C-T, et al. J Polym Res 2014;21:338.
[8] Report N 1, Thermal insulation materials made of rigid polyurethane foam (PUR/PIR), properties-manufacture. Federation of European Rigid Polyurethane Foam Association; 2006.
[9] Minges ML. Thermal insulations for aerospace applications: −423°F to +3000°F, lst Lt, USAF. Technical Documentary Report ASD-TDR-63–699. 1963.
[10] Papadopoulos AM. State of the art in thermal insulation materials and aims for future developments. Laboratory of Heat Transfer and Environmental Engineering, Department of Mechanical Engineering, Aristotle University Thessaloniki, Greece.
[11] Gibson LJ, Ashby MF. Cellular solids, structure and properties. Pergamon Press; 1988.
[12] Venkatesan G, Macosko CW, Choi JH, Bischof J. J Cell Plast 2008;44:481–91.
[13] Skochdopole RE. Eng Prog 1961:57.
[14] Hilyard NC, Cunningham A. Low density cellular plastics. 1994.
[15] Glicksman LR, Schuetz M, Sinoftsky M. Int Heat Mass Transf 1987;30:187–97.
[16] Gupta N, Ricci W. J Mat Process Techn 2008;198:178–82.
[17] Baetensa R, Jelle BP, Gustavsend A. Energy Build 2011;43:761–9.
[18] Tseng C-j, Yamaguchi M, Ohmori T. Cryogenics 1997;37:305–12.
[19] Meador MAB, Lyn C, McCorkle A, Papadopoulos L, Demetrios S, Leventis N. Chem Mater 2007;19:2247–60.
[20] Kanamori K, Aizawa M, Nakanishi K, Hanada T. J Sol-Gel Sci Technol 2008;48:172–81.
[21] Tokudome Y, Nakanishi K, Kanamori K, Fujita K, Akamatsu H, Hanada T. J Colloid Interface Sci 2009;338:506–13.
[22] Wingfield C, Franzel L, Bertino MF, Leventis N. J Mater Chem 2011;21:11737–41.
[23] Yoldas BE, Annen MJ, Bostaph J. Chem Mater 2000;12:2475–84.
[24] Oh KW, Kim DK, Kim HS. Fibers Polym 2009;10(5):731–7.
[25] Okoroafor MO, Wang AE, Yoldas BE. WO 1996000750 A1.
[26] Zou K, Soucek MD. Macromol Chem Phys 2004;205:2032–9.
[27] Brinker CJ, Scherer GW. Sol-gel science: the physics and chemistry of sol-gel processing. 1992.
[28] Pauw BR. J Phys Condens Matter 2013;25:38.
[29] Yano S, Iwata K, Kurita K. Mater Sci Eng C 1998;6:75.
[30] ASTM D 1621 − 04a. Standard test method for compressive properties of rigid cellular plastics1.
[31] Glaser RH, Wilkes GL, Bronnimann CE. J Non-Crystalline Solids 1989;113:73–87.
[32] Lippmaa E, Matgi M, Samoson A, Engelhardt G, Grimmer AR. J Am Chem Soc 1980;102:4889.
[33] Piscitelli F, Lavorgna M, Buonocore GG, Verdolotti L, Galy J, Mascia L. Macromol Mat Eng 2013;298(8):896–909.
[34] Beaucage G, Ukibarri TA, Black EP, Schaefer DW. In: Mark JE, Lee CYC, Bianconi PA, editors. Hybrid organic-inorganic composites. Washington, DC: ACS; 1995.
[35] Zaioncz S, Dahmouche K, Soares BG. Macromol Mat Eng 2010;295:243–55.
[36] Xiong M, Zhou S, Wu L, Wang B, Yang L. Polymer 2004;45:8127–38.
[37] Xia Y, Larock RC. Macromol Rapid Commun 2011;32:1331–7.
[38] Biesmans G, Randall D, Francais E, Perrut M. J Non-Crystalline Sol 1998;225:36–40.
[39] Verdolotti L, Lavorgna M, Di Maio E, Iannace S. Poly Degr Stab 2013;98(1):64–72.
[40] Nikje MMA, Garmarudi AB, Haghshenas M, Mazaheri Z. Nanotechnology in construction. 2009. p. 149–54.
[41] Verdolotti L, Di Maio E, Forte G, Lavorgna M, Iannace S. J Mater Sci 2010;45:3388–91.